Article

Synthesis, Crystal Structures and Phase Transitions of Dabco Oxonium Triperchlorate and Tritetrafluoroborate

Marek Szafra#ski

Cryst. Growth Des., **Just Accepted Manuscript** • DOI: 10.1021/acs.cgd.8b01282 • Publication Date (Web): 01 Oct 2018

Synthesis, Crystal Structures and Phase Transitions of Dabco Oxonium Triperchlorate and Tritetrafluoroborate

Marek Szafrański*

Faculty of Physics, Adam Mickiewicz University, Umultowska 85, 61-614 Poznań, Poland;

e-mail: masza@amu.edu.pl

Abstract: Complexes of $(C_6H_{14}N_2)H_3O(ClO_4)_3$ and $(C_6H_{14}N_2)H_3O(BF_4)_3$ crystallize from strongly acidic water solutions of 1,4-diazabicyclo[2.2.2]octane. The crystals have been characterized by thermogravimetric analysis, differential scanning calorimetry, X-ray diffraction, dilatometry, and dielectric studies. Four crystalline phases of the perchlorate complex have been identified. Their highly-symmetric cubic structures are diversified by the degree of structural disorder. The first-order transition to the highly disordered high-temperature phase I at 387.8 K is associated with a huge entropy gain of 29.3 $Jmol^{-1}K^{-1}$, and a jump-wise expansion of the crystal by 1.4%. The second-order transition at 295.8 K, between phases II and III, has also an order-disorder character and it is associated with an unusual dielectric response related to the dipolar fluctuations induced be ordering of the oxonium cations. Phase III of the crystal transforms to the low-temperature phase IV through the first-order transition around 127 K. The terafluoroborate complex crystallizes in a topologically distinct structure of hexagonal symmetry. The crystal undergoes a second-order phase transition at 335 K. Although, the transition entropy of 30 $Jmol^{-1}K^{-1}$ clearly indicates an order-disorder mechanism, the low-temperature phase II remains partly disordered even at 100 K. The substantial differences between the structures and properties of both compounds have been attributed to the different properties of the ClO_4^-/BF_4^- ions and of the O–H···O/O–H···F hydrogen bonds.

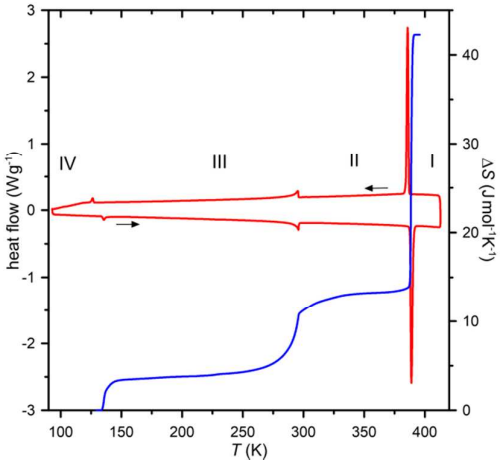

*Marek Szafrański
phone: + 48 61 8295094
fax: + 48 61 8295155
e-mail: masza@amu.edu.pl

Synthesis, Crystal Structures and Phase Transitions of Dabco Oxonium Triperchlorate and Tritetrafluoroborate

Marek Szafrański*

Faculty of Physics, Adam Mickiewicz University, Umultowska 85, 61-614 Poznań, Poland;

Abstract: Complexes of $(C_6H_{14}N_2)H_3O(ClO_4)_3$ and $(C_6H_{14}N_2)H_3O(BF_4)_3$ crystallize from strongly acidic water solutions of 1,4-diazabicyclo[2.2.2]octane. The crystals have been characterized by thermogravimetric analysis, differential scanning calorimetry, X-ray diffraction, dilatometry, and dielectric studies. Four crystalline phases of the perchlorate complex have been identified. Their highly-symmetric cubic structures are diversified by the degree of structural disorder. The first-order transition to the highly disordered high-temperature phase I at 387.8 K is associated with a huge entropy gain of 29.3 $Jmol^{-1}K^{-1}$, and a jump-wise expansion of the crystal by 1.4%. The second-order transition at 295.8 K, between phases II and III, has also an order-disorder character and it is associated with an unusual dielectric response related to the dipolar fluctuations induced be ordering of the oxonium cations. Phase III of the crystal transforms to the low-temperature phase IV through the first-order transition around 127 K. The terafluoroborate complex crystallizes in a topologically distinct structure of hexagonal symmetry. The crystal undergoes a second-order phase transition at 335 K. Although, the transition entropy of 30 $Jmol^{-1}K^{-1}$ clearly indicates an order-disorder mechanism, the low-temperature phase II remains partly disordered even at 100 K. The substantial differences between the structures and properties of both compounds have been attributed to the different properties of the ClO_4^-/BF_4^- ions and of the O–H···O/O–H···F hydrogen bonds.

Keywords: dabco, oxonium ion, phase transition, disorder, entropy

INTRODUCTION

Two nitrogen atoms of 1,4-diazabicyclo[2.2.2]octane molecule ($C_6H_{12}N_2$, dabco) can serve as the proton-acceptor sites, and therefore in the reactions with acids this organic base is prone to form complexes of different stoichiometry.[1] The most intensely have been studied the 1:1 complexes of dabco with monoprotic acids, where the monoprotonated cations are hydrogen bonded into linear chains.[1-7] This unique arrangement of the cations and the behaviour of protons in the N–H···N hydrogen bonds are crucial for the properties of these compounds. The room-temperature ferroelectricity of dabco tetrafluoroborate,[4] dabcoHBF$_4$, and dabco perchlorate,[4] dabcoHClO$_4$, is associated with ordered protons in the antiparallel polarized polycationic chains, while in the analogous dabco perrhenate,[5] dabcoHReO$_4$, the ordered hydrogen bonds are parallel, and thus contribute substantially to the total polarization of the crystal. The disorder of protons in the N–H···N hydrogen bonds in dabco hydroiodide, dabcoHI, hydrobromide, dabcoHBr, and dabco hydrochloride trihydrate, dabcoHCl·3H$_2$O, results in a new property of unprecedented one-dimensional dielectric response, resembling relaxor ferroelectricity.[6,8,9] It was evidenced that the protons disorder can persists to the temperatures as low as 1.5 K.[10] The formation of linear polycationic $(dabcoH^+)_n$ chains was also observed in a molecular semiconductor (dabcoH)$_2$(TCNQ)$_3$[11] and in an organic-organometallic salt (dabcoH)[Re$_2$(μ-OMe)$_3$(CO)$_6$].[12] The self-assembling of dabco cations into chains is remarkable in this respect that hydrogen bonds are formed between the positively charged ions, while usually they link the ions of opposite charges.[7] A more conventional system of hydrogen bonds is observed in the complexes where dabco adopts a diprotonated form, $(dabcoH_2)^{2+}$.[13-16] The 1:2 complexes of dabco with the perchloric and tetrafluoroboric acids crystallize as hydrates, (dabcoH$_2$)(BF$_4$)$_2$·H$_2$O and (dabcoH$_2$)(ClO$_4$)$_2$·H$_2$O. Although their room-temperature phases are polar, these crystals do not exhibit ferroelectricity, but they undergo ferroelastic phase transitions.[16] Herein we show that by changing the acidity of the stoichiometric 1:2 aqueous solutions, new materials of cationic sublattices formed from divalent $(dabcoH_2)^{2+}$ and monovalent oxonium H_3O^+ cations can be obtained. The synthesis and the crystal structures of dabco oxonium triperchlorate, (dabcoH$_2$)H$_3$O(ClO$_4$)$_3$ and dabco oxonium tritetrafluoroborate, (dabcoH$_2$)H$_3$O(BF$_4$)$_3$, are described. We characterise also the phase transitions and dielectric properties of these compounds.

EXPERIMENTAL DETAILS

Dabco and 70% $HClO_4$ or 40% HBF_4 were dissolved in water in stoichiometric ratio 1:2. The concentrated solutions were strongly acidified with an excess of $HClO_4$/HBF_4 and left at room temperature for crystallization. The colourless crystals formed during a couple of weeks were identified by single-crystal X-ray diffraction as $(dabcoH_2)H_3O(ClO_4)_3$ and $(dabcoH_2)H_3O(BF_4)_3$, respectively.

Thermal stability of the crystals was studied by thermogravimetric analysis (TGA) with a TGA Q50 instrument (TA Instruments). The polycrystalline samples were heated in nitrogen atmosphere at a temperature rate of 10 K/min.

Calorimetric measurements were carried out by differential scanning calorimetry (DSC) using a Q2000 calorimeter (TA Instruments). The DSC cooling/heating runs were measured on the powdered samples at a rate of 10 K/min. Pure indium standard was used for the temperature and enthalpy calibration as well as synthetic sapphire for specific heat calibration.

Studies of the relative complex electric permittivity $\varepsilon = \varepsilon' - i\varepsilon''$ were performed on the pressed pellets or oriented single-crystal plates with gold electrodes deposited by sputtering. The real part of electric permittivity and dielectric loss were measured in the frequency range from 1 kHz to 8 MHz with a Hewlett-Packard 4192A impedance analyser, at the amplitude of the ac measuring electric field of about 3 V/cm. The temperature of the sample was changed at a rate of 0.5 K/min.

The single-crystal X-ray diffraction studies were performed with an Oxford Diffraction Gemini A Ultra diffractometer operating with graphite-monochromated Mo$K\alpha$ radiation. The CrysAlis^{Pro} software[17] was used for the data collection and processing. The data were collected at different fixed temperatures in the temperature range between 100 and 400 K. The crystals were cooled/heated with a Cryostream Plus (Oxford Cryosystems) attachment. The temperature of the nitrogen stream was stabilized within ±0.3 K. The crystal structures were solved with direct methods using SHELXS97 and refined by full-matrix least-squares method on all intensity (F^2's) data with SHELXL97.[18] Experimental and final structural details are collected in Table 1. Crystallographic information files have been deposited in the Cambridge Crystallographic Database Centre as CCDC nos. 1862850–1862854.

Table 1. Selected crystallographic and refinements data for the structures of $(dabcoH_2)H_3O(ClO_4)_3$ in phases I, II and III and $(dabcoH_2)H_3O(BF_4)_3$ in phases I and II.

Crystal formula	$C_6H_{17}N_2O_{13}Cl_3$			$C_6H_{17}B_3F_{12}N_2O$	
Phase	III	II	I	II	I
Temperature (K)	200.0(1)	310.0(1)	400.0(2)	100.0(3)	340.0(3)
Crystal system	cubic			hexagonal	
Space group	$P2_13$	$Pa\bar{3}$	$Fm\bar{3}c$	$P6_3/m$	$P6_3/mmc$
Unit cell a (Å)	14.28590(13)	14.34001(19)	14.5212(3)	10.0090(5)	10.2557(7)
c (Å)				8.0565(7)	8.3873(9)
Volume (Å^3)	2915.57(5)	2948.82(7)	3062.03(12)	698.97(8)	763.98(11)
Z	8	8	8	2	2
ρ (g cm^{-3})	1.966	1.944	1.872	1.870	1.711
μ (mm^{-1})	0.707	0.699	0.673	0.226	0.207
Reflections collected/unique	5679 / 2323	4630 / 1169	635 / 178	1771/682	1640/374
R_{int}	0.0265	0.0329	0.0336	0.0166	0.0307
R_1/wR_2 ($I>2\sigma_I$)	0.0280 / 0.0626	0.0297 / 0.0735	0.0310 / 0.0789	0.1372/0.3654	0.1374/0.3418
R_1/wR_2 (all data)	0.0350 / 0.0640	0.0453 / 0.0772	0.0391 / 0.0868	0.1523/0.3764	0.2020/0.3655
Peak/hole (e Å^{-3})	0.263 / -0.402	0.245 / -0.406	0.209 / -0.207	1.248/-1.216	0.535/-0.207
Flack parameter	0.43(7)	-	-	-	-

RESULTS AND DISCUSSION

Thermal Stability. TGA measurements (Figure S1a) show that $(dabcoH_2)H_3O(ClO_4)_3$ is stable in the temperature range up to about 420 K. Above this temperature the substance starts to decompose before reaching the melting point. The thermal stability region of $(dabcoH_2)H_3O(BF_4)_3$ is limited to about 375 K (Figure S1b). All further studies were carried out within the thermal stability region of the crystals.

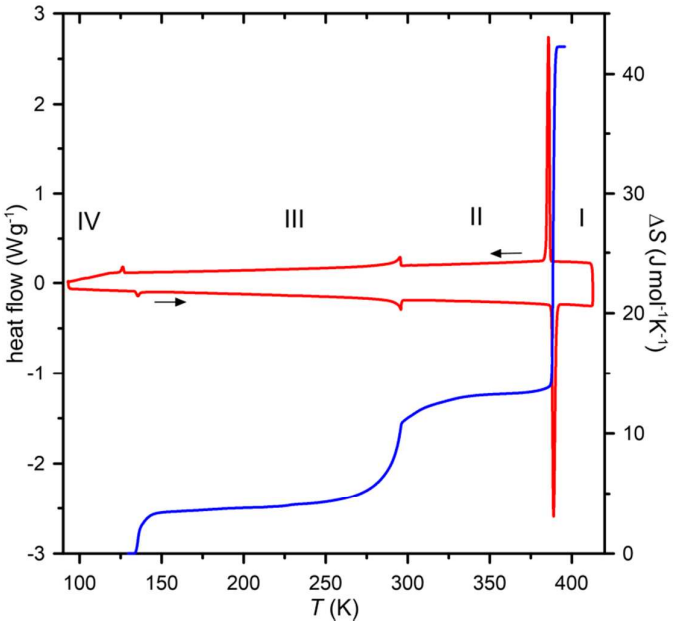

Figure 1. The cooling and heating DSC runs (left axis) and the entropy changes (right axis) across the phase transitions of $(dabcoH_2)H_3O(ClO_4)_3$.

Calorimetric Study of $(dabcoH_2)H_3O(ClO_4)_3$. The results of calorimetric measurements plotted in Figure 1a indicate four crystalline phases of $(dabcoH_2)H_3O(ClO_4)_3$, which are labelled by Roman numbers I, II, III and IV, starting from the high-temperature phase. The transition between phases I and II is visibly of first-order, despite of the only small temperature hysteresis of about 1 K between the transition temperature in the cooling and heating runs (T_{12} = 386.8 K and T_{21} = 387.8 K). The transition is associated with the enthalpy change ΔH_{21} = 11.4 kJmol^{-1} and the transition entropy ΔS_{21} = 29.3 Jmol^{-1}K^{-1}. A comparison of this huge entropy gain to $R\ln N_1/N_2$ (where R is the gas constant, and N_1, N_2 are the numbers of configurations in phases I and II) gives the ratio $N_1/N_2 = 34$, indicating a strongly order-disorder character of the transition. The next thermal anomaly observed close to the room temperature is attributed to the transition between phases II and III. This anomaly is characterized by a lack of temperature hysteresis ($T_{23} = T_{32} = 295.8$ K) and its shape is characteristic of the second-order phase transitions. The total entropy change ΔS_{32} was estimated from the $C_p(T)$ dependence (Figure S2) according to the formula $\Delta S = \int_{T_1}^{T_2}\left[C_p(T) - C_b(T)\right]/T dT$, where $C_b(T)$ is the baseline and T_1, T_2 are the limits of the thermal anomaly integration. The calculated entropy change ΔS_{32} = 9.0 Jmol^{-1}K^{-1} ($\approx R$ ln3) strongly suggests that also this transition is of an order-disorder type. In the low-temperature region

$(dabcoH_2)H_3O(ClO_4)_3$ undergoes yet another phase transition at T_{34} = 127 K on cooling and at T_{43} = 134 K on heating. The large temperature hysteresis of 7 K and the shape of thermal anomaly testify to a first-order nature of this transition. The enthalpy change ΔH_{43} = 442 $Jmol^{-1}$ and the corresponding entropy gain ΔS_{43} = 3.3 $Jmol^{-1}K^{-1}$ ($\approx R\ln 1.5$) suggest a displacive mechanism of this transition.

Crystal Structures and Mechanism of Phase Transitions in $(dabcoH_2)H_3O(ClO_4)_3$. The structure of the room-temperature phase III of $(dabcoH_2)H_3O(ClO_4)_3$ is highly symmetric of space group $P2_13$ (Table 1). The packing of the ions in the unit cell is shown in Figure 2a. The cohesion forces of the crystal are dominated by the electrostatic attraction between the cations and anions. Apart from the electrostatic forces the structure is also stabilized by O–H···O hydrogen bonds linking the oxonium cations to the perchlorate anions and by N–H···O bonds between the dabco dications and the anions. There are two symmetry independent oxonium cations, both situated on the 3-fold symmetry axes in the octahedral voids formed of six ClO_4^- tetrahedra. The nearest surrounding of the oxonium cations is pictured in Figures 2b and S3. Within the voids the H_3O^+ cations are located off-center due to the interaction through the hydrogen bonds with the oxygen atoms of the surrounding anions. At 200 K the oxonium cation 1s (labelled according to the oxygen atom O1s) has a pyramidal shape with H1s–O1s–H1s angle of 114.7° and it is tied to the ClO_4^- tetrahedra by three hydrogen bonds with the distances O1s···O4 of 2.629(2) Å (Figure 2b). In the nearest surrounding of this cation there are also three alternative proton-acceptor oxygen atoms, but of substantially longer distances O1s···O8 of 2.849(2) Å. The second oxonium cation 2s is a bit less flattened with H2s–O2s–H2s pyramidal angle of 113.7°. This correlates with the slightly weaker hydrogen bonds (O2s···O5 = 2.692(2) Å linking the cation to the ClO_4^- anions. In this case the next nearest proton-acceptor oxygen atoms O1(3x) and O2(3x) are situated respectively 3.048(3) and 3.035(3) Å from O2s. Thus, the formation of alternative hydrogen bonds is unlikely, especially in low temperatures. The ordering of both H_3O^+ cations at 200 K is confirmed by the positions of hydrogen atoms located from the difference Fourier maps.

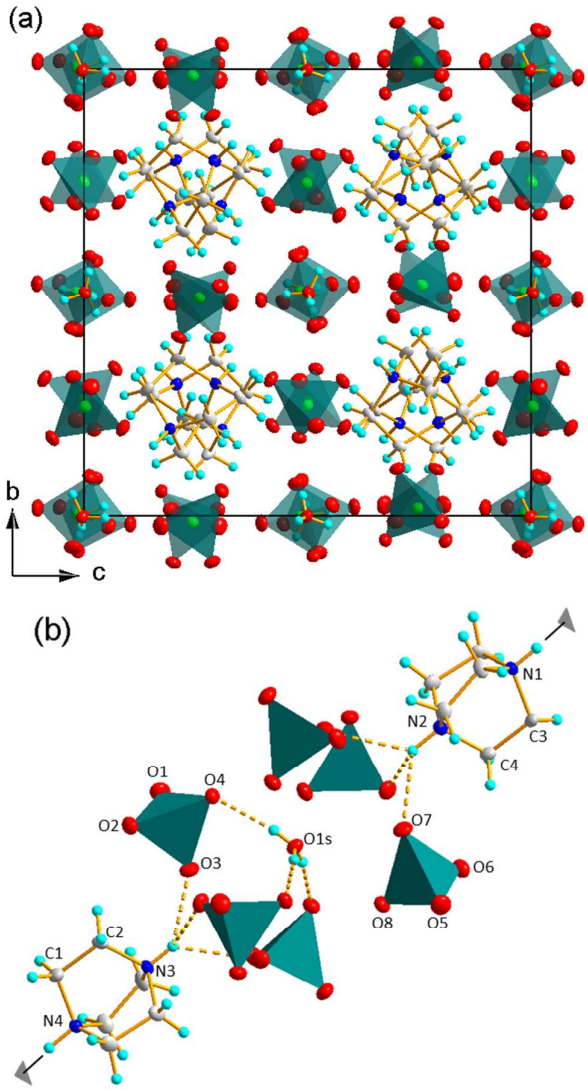

Figure 2. Crystal structure of $(dabcoH_2)H_3O(ClO_4)_3$ phase III at 200 K viewed along [100] (a) and the nearest surrounding of the oxonium cation 1s, illustrating the arrangement of the ions and hydrogen bonds around the 3-fold symmetry axis (b). Thermal ellipsoids of the heavy atoms are drawn at 50% probability level, the dashed lines illustrates the H-bonds.

The diprotonated $dabcoH_2^{2+}$ cations occupy sites on the 3-fold symmetry axes (see Figures 2b and S2). This site symmetry is consistent with the symmetry of the ordered cation. The positions of the $dabcoH_2^{2+}$ cations are stabilized by weak N–H···O hydrogen bonds with distances N···O between 2.982 and 3.107 Å. In phase III the ethylene bridges $–CH_2–CH_2–$ are twisted resulting in the propeller-like conformation. At 200 K the torsional angles C–N–N–C are close to 10.5^o in both symmetry independent cations.

The transition between the phases III and II has a continuous character, and accordingly the symmetry change $Pa\bar{3} \rightarrow Fm\bar{3}c$ fulfil a subgroup-group relation. An excess of the proton-acceptor sites in the nearest surrounding of the H_3O^+ ions creates conditions for the formation of the alternative hydrogen bonds. However, this requires breaking of the existing O–H···O bonds, as well as the rotation and tumbling of the whole H_3O^+ pyramid. A partial disorder of the oxonium cations can be inferred from an anomalous increase of the crystal entropy in phase III about 50 K below the transition point at T_{32}, as shown in Figure 1.

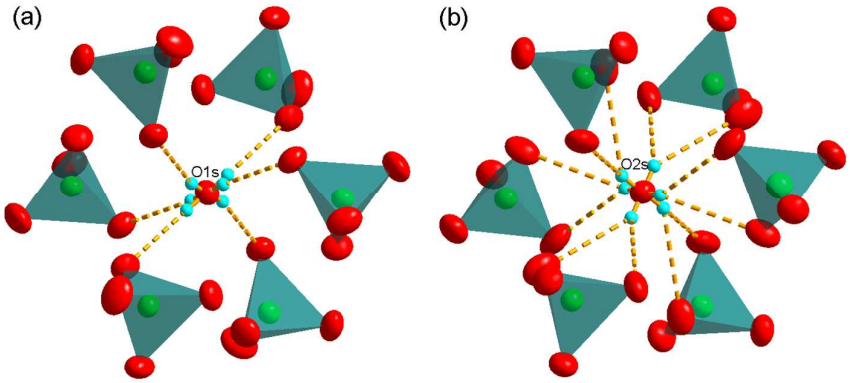

Figure 3. Two symmetry independent oxonium cations 1s (a) and 2s (b) in phase II of $(dabcoH_2)H_3O(ClO_4)_3$ at 310 K. The O–H···O hydrogen bonds linking the disordered H_3O^+ pyramids to the ClO_4^- tetrahedra are drawn by dashed lines.

The activation of the H_3O^+ hopping between the two sites in the voids formed by the ClO_4^- tetrahedra leads ultimately to the crystal lattice symmetry change at the transition to phase II. In phase II both disordered oxonium cations occupy central positions in the voids at the inversion centers, but they are involved in the different systems of hydrogen bonds (Figure 3). The cation 1s is tied by two equivalent sets of hydrogen bonds, each composed of three O–H···O bonds. These bonds have the same geometry and O···O distances of 2.745 Å. The second oxonium cation 2s is linked by six hydrogen bonds in each of the two disordered sites. Each hydrogen atom is involved in a couple of bifurcated bonds with distances O2s···O1 of 2.985 Å and O2s···O3 of 3.005 Å. In phase II there is only one symmetry independent $dabcoH_2^{2+}$ cation, which remains ordered at 310 K and retains the propeller-like conformation with the torsion angle N1–C3–C2–N2 of 14.1°.

The raising of temperature in phase II results in an additional contribution to the entropy above c.a. 350 K in Figure 1. This indicates the activation of a new mode of structural disorder, which is most probably related to $dabcoH_2^{2+}$. Above the transition point at T_{21} this

cation is strongly disordered due to the rotations and/or tumbling motions about the center of gravity (Figure 4). In phase I the crystal adopt the high symmetry of space group $Fm\bar{3}c$ (Table 1). As a consequence the disordered oxonium cations acquire the same properties, as all they occupy the centres of identical octahedral voids being involved in twelve weak hydrogen bonds with O···O distances of 3.032 Å.

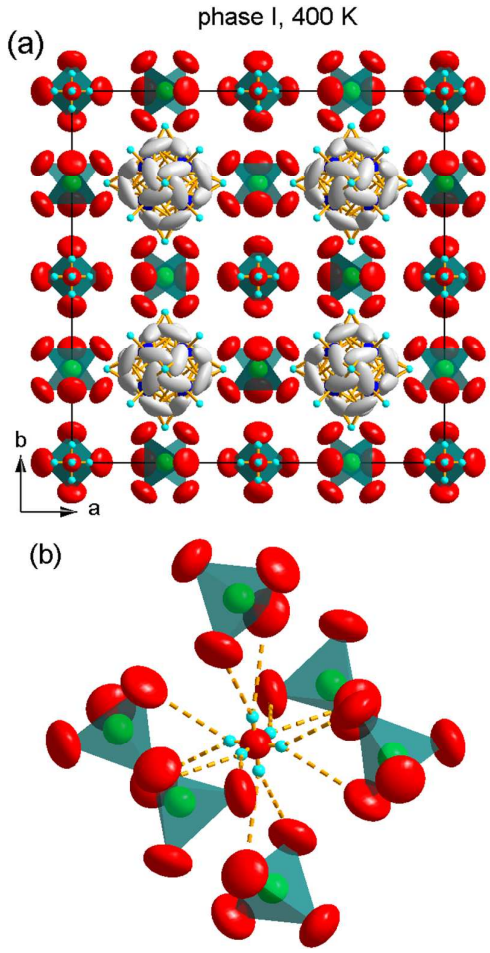

Figure 4. The crystal structure of $(dabcoH_2)H_3O(ClO_4)_3$ (a) and the octahedral surrounding of the disordered oxonium cation (b), in phase I at 400 K.

Thermal Expansion of $(dabcoH_2)H_3O(ClO_4)_3$. In the phases I, II and III the $(dabcoH_2)H_3O(ClO_4)_3$ crystals maintain the cubic symmetry, and the transition to the low-temperature phase IV seems to occur also within the cubic system, judging by the unit-cell dimensions. However, the refinements of the structure in the most probable cubic space groups failed. Also, no satisfactory model was obtained for the lower symmetries tested.

Therefore, this issue remains open as the crystal in phase IV may be subtly twinned due to the possible pseudo-cubic lattice.

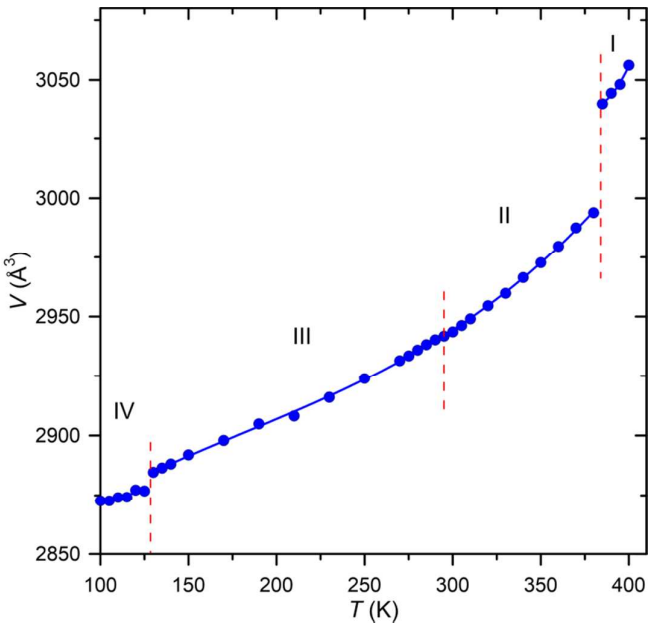

Figure 5. Temperature dependence of the unit-cell volume of $(dabcoH_2)H_3O(ClO_4)_3$ across the phases I-IV.

The thermal expansion of the cubic lattice parameter is plotted in Figure S4, while the corresponding temperature dependence of the unit-cell volume is shown in Figure 5. These plots clearly demonstrate the continous character of the transition between phases II and III, as well as the discontinous changes at the first-order transitions between phases I and II, and between phases III and IV. Noteworthy is a large change in the unit-cell volume at T_{21}, where the crystal expands by 1.4%. Through the Clausius-Clapeyron equation $dT/dp = \Delta V/\Delta S$ it is possible to estimate the pressure coefficient of the transition temperature. The unit-cell volume jump $\Delta V_{21} = 42$ Å^3 and the transition entropy $\Delta S_{21} = 29.3$ Jmol^{-1}K^{-1}(67.9 J kg^{-1}K^{-1}) correspond to the pressure coefficient $dT_{21}/dp = 108$ K GPa^{-1}. It is noteworthy that the transitions associated with large entropy gain and strong pressure dependence of the transition temperature are sought because of potential applications for energy storage and solid-state cooling.[20,21]

Dielectric properties of $(dabcoH_2)H_3O(ClO_4)_3$. The phase transitions in $(dabcoH_2)H_3O(ClO_4)_3$ are associated with anomalies in the dielectric properties of the crystal (Figure 6). Particularly interesting are the changes in the electric permittivity at the

continuous phase transition between phases III and II. The real part, ε', of the complex electric permittivity forms a large peak with a maximum at the transition point, which resembles the anomalies observed at the ferroelectric-paraelectric phase transitions.[19] However, the high-temperature slope of the anomaly does not fulfil the Curie-Weis law, and no ferroelectric hysteresis loop was detected in phase III. This excludes the crystal ferroelectricity, which is consistent with the cubic symmetry of both phases determined from the single-crystal X-ray diffraction study. The outstanding dielectric response in the vicinity of T_{32} can be escribed to critical fluctuations of the order parameter. The contribution of such fluctuations to the entropy change is clearly seen in Fig. 1a above the transition point in phase II. At a microscopic level the formation and disappearance of the ordered polar clusters (see Figure 2b) results from the hopping of the oxonium ions. This generates fluctuations of the local electric dipole moments, giving a substantial contribution to the electric permittivity.

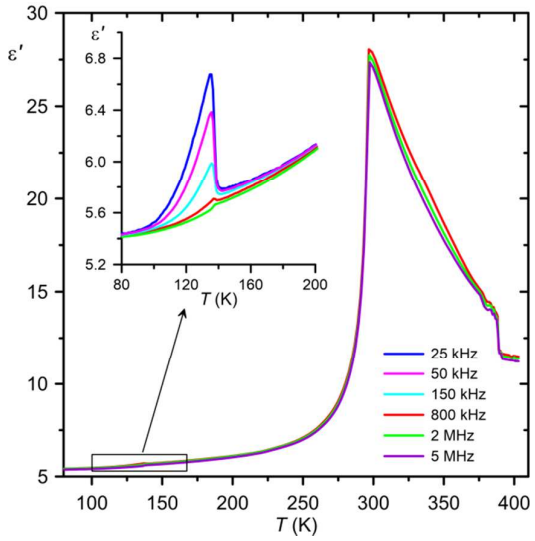

Figure 6. Temperature dependence of the real part of electric permittivity of the polycrystalline $(dabcoH_2)^{2+}H_3O^+(ClO_4^-)_3$ sample measured in the heating run for different frequencies of electric field.

The transition to the high-temperature phase I is seen in Figure 6 as a drop in the electric permittivity. However, it should be stressed that the magnitude of this drop differed significantly for different samples and runs. Therefore, it is highly probable that this was mainly due to a worsening of the contacts between the electrodes and the sample when the crystal phase II transformed to phase I. This is a consequence of a huge lattice expansion at the transition point, which is evident from the $V(T)$ plot in Figure 5.

Although relatively small, but interesting changes in the dielectric properties of the crystal are observed at the transition to the low-temperature phase IV. The inset in Figure 6 shows that the real part of electric permittivity is strongly frequency-dependent in phase IV. Also the magnitudes of the step-wise changes at T_{43} strongly depend on the frequency. The substantial increase of ε' in phase IV just below the transition point, especially pronounced for low frequencies in the kilohertz range, seems to be very unusual. The frequency dispersion in this temperature region was also observed in the dielectric losses (Figure S5). These results indicate that a dielectric relaxation process takes place in phase IV and it is supressed when the crystal transforms to phase III. Thus, the strong frequency dependence of ε' at the transition temperature results from a cut-off of the dipolar relaxation, which is caused by the transformation of the crystal structure.

Calorimetric study of $(dabcoH_2)H_3O(BF_4)_3$. The DSC study revealed a continuous phase transition in $(C_6H_{14}N_2)H_3O(BF_4)_3$ at T_{21} = 335 K (Figure 7). The transition is associated with a huge entropy change ΔS_{21} = 30 $Jmol^{-1}K^{-1}$, corresponding to R ln 37. This indicates that the high-temperature phase I is strongly disordered. From the plots in Figure 7 it is apparent

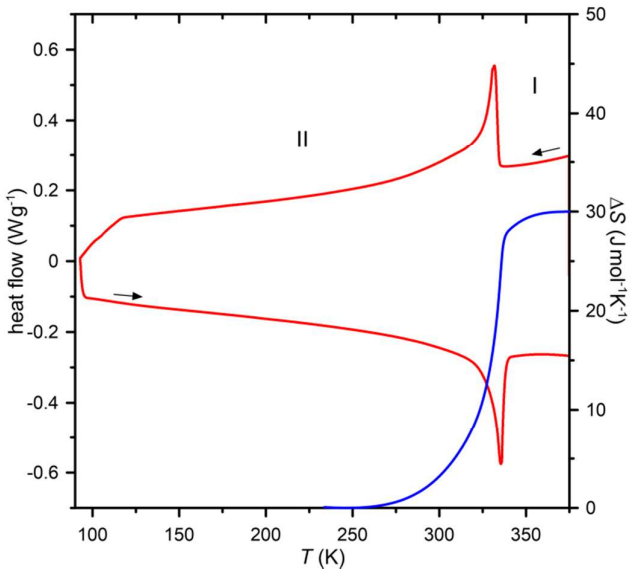

Figure 7. The cooling and heating DSC runs (left axis) and the entropy changes (right axis) in the vicinity of the second-order phase transition in $(dabcoH_2)H_3O(BF_4)_3$.

that the process of disordering starts in phase II about 80 K below the transition point, and it grows progressively until the crystal transformation to the phase I.

Crystal Structure and Machanism of phase transition in $(dabcoH_2)H_3O(BF_4)_3$. The high entropy gain accompayning the transition in $(dabcoH_2)H_3O(BF_4)_3$ is consistent with the strongly disordered structural model of phase I. The structure of this phase was solved and

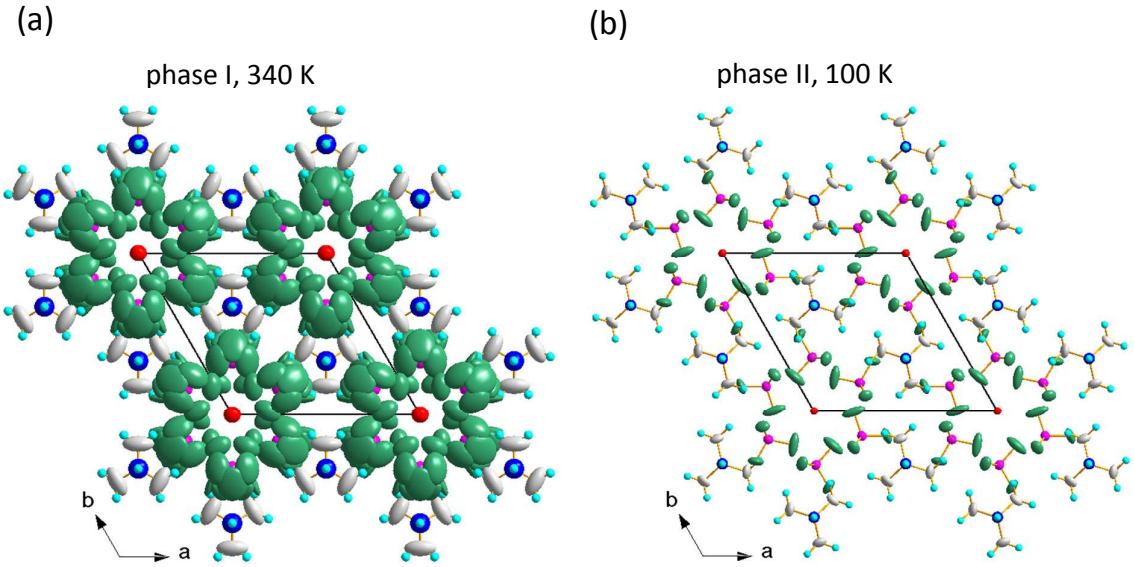

Figure 8. Crystal structures of $(dabcoH_2)H_3O(BF_4)_3$ in phase I at 340 K (a) and in phase II at 100 K, viewed along the hexagonal axes. The thermal elipsoids have been drawn at the 50% probability level. Color codes: B – magenta, F – green, O – red, C – gray, N – blue, H – light blue.

refined in hexagonal space group $P6_3/mmc$. As shown in Figure 8a the tetrafluoroborate anions are disordered and arranged along [z] in a form of hexagonal channels. The disorder of BF_4^- was modeled with 16 partly occupied sites of the fluorine atoms located around the anion center of gravity. However, the large thermal elipsoids of the atoms situated at the disordered sites suggest that the anion can perform rotations aroud the central B atom. The oxonium cations are situated in the channels, at the sites of symmetry $\bar{3}m$, having six equidistant BF_4^- anions in the nearst surrounding. This indicates a possibility of breaking and formation of the alternative O–H···F hydrogen bonds, and in a consequence the disordering of the OH_3^+ cations. Accordingly, the split sites of the hydrogen atoms can explain the impossibility of their location from the difference Fourier maps. The arrangement of the diprotonated dabco cations well fits in the hexagonal motif of the crystal structure. Six pillars composed of $dabcoH_2^{2+}$ surround every BF_4^- hexagonal channel when the structure is viewed along [z] as in Figure 8. The cations occupy sites of 3*m* symmetry with their 3-fold symmetry axes paralel to [z]. The large thermal elipsoids of C atoms, elongated perpendicular to the N–C bonds,

indicate that the dabco cations perform large-amplitude vibrations or rotations around their 3-fold symmetry axes.

On cooling phase I of $(dabcoH_2)H_3O(BF_4)_3$ transforms continuously to phase II at T_{21} = 335 K, and the crystal symmetry lowers from $P6_3/mmc$ to $P6_3/m$. This symmetry change satisfies a group-subgroup relation required for the second-order phase transitions. The reduction of symmetry is due to the ordering of the structure in phase II, which starts at the transition and proceeds continuously with lowering the temperature. The refinement of the structure at 100 K indicates that phase II is not completely ordered even in a such low temperature. Some residual disorder can be infered from the relatively large thermal elipsoids of the fluorine atoms of the BF_4^- tetrahedra. Moreover, in phase II the oxonium cations occupy sites of symmetry $\bar{3}$, and therefore they have to be disordered also in this phase. This conclusion is justified by the six equivalent sites for the three hydrogen atoms in the hydrogen bonds O–H···F (O···F distance of 2.958 Å). The disorder of OH_3^+, either dynamic or static, concerns only the hydrogen atoms, making their location difficult, whereas the oxygen atoms occupy well defined sites, as evidenced by their small thermal elipsoids (Figure 8b). The disorder in phases I and II make hard the refinements of the structures and can be one of the reasons responsible for the relatively high reliability *R*-factors (see Table 1). The other cause can be a merhoedral twinning of the crystal, although our attempts to model such twinning failed. Similarly, the refinements of the low-temperature structure in the lower-symmetry space groups proved unsuccessful. It is also worth noticing that the structural data were collected on numerous samples from different crystallizations, and all the crystals used in the X-ray diffraction experiments produced good diffraction patterns with narrow Bragg reflections.

Thermal Expansion of $(dabcoH_2)H_3O(BF_4)_3$. The second-order character of the transition between phases I and II is testified by the continuous changes of the unit-cell parameters and volume as a function of temperature (Figure 9). The nonlinear thermal expansion of the crystal in phase II can be correlated with the anomalous entropy changes (Figure 7) related to the temperature-activated structural disorder. The $V(T)$ dependence, plotted in Figure 9, allowed us to determine the volume thermal expansion coefficient, α_V, in both phases of the crystal (Figure S6), and to estimate the change of this coefficient at the transition point, $\Delta\alpha_V = 1.45 \cdot 10^{-3}$ K^{-1}. By applying the Ehrenfest's relation, $dT/dp = T_0V_0\Delta\alpha_V/\Delta C_p$, where V_0 is the crystal volume at the transition temperature T_0, and ΔC_p is the specific heat difference between the phases II and I at T_0, it is easy to estimate the pressure coefficient of the

transition. Having $\Delta C_p = 735.5$ J mol^{-1} K^{-1} determined from the DSC measurements we calculated $dT_{21}/dp = 151$ K GPa^{-1}. This estimation predicts a strong pressure dependence of the transition temperature T_{21}.

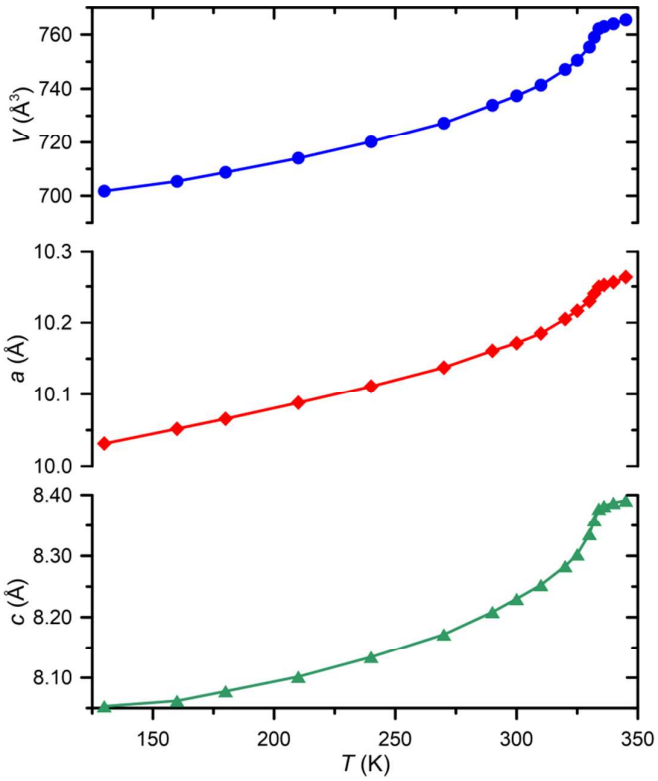

Figure 9. Lattice parameters and unit-cell volume of $(dabcoH_2)H_3O(BF_4)_3$ as a function of temperature.

Dielectric properties of $(dabcoH_2)H_3O(BF_4)_3$. The transition in $(dabcoH_2)H_3O(BF_4)_3$ is associated with an anomalous dielectric response of the crystal. The real part of the relative electric permittivity, ε', assumes relatively high values of above 10, even in the temperatures 100 K below the transition point (Figure 10). Moreover, ε' increases progressively as the temperature grows, starting from about 250 K, which well corresponds to the activation of the structural disorder in the crystal lattice. The dynamical disorder of the ions results also in an increase in the dielectric losses (Figure S7), and causes a rising frequency dispersion of the dielectric components ε' and ε'', with increasing temperature. Although the dynamics of the ions evidently contributes to the dielectric response of $(dabcoH_2)H_3O(BF_4)_3$, the character of the anomaly at the transition between phases II and I is substantially different from that

accompanying the transition between phases III and II in the analogous $(dabcoH_2)H_3O(ClO_4)_3$. Both these transitions are continuous and they involve the order-

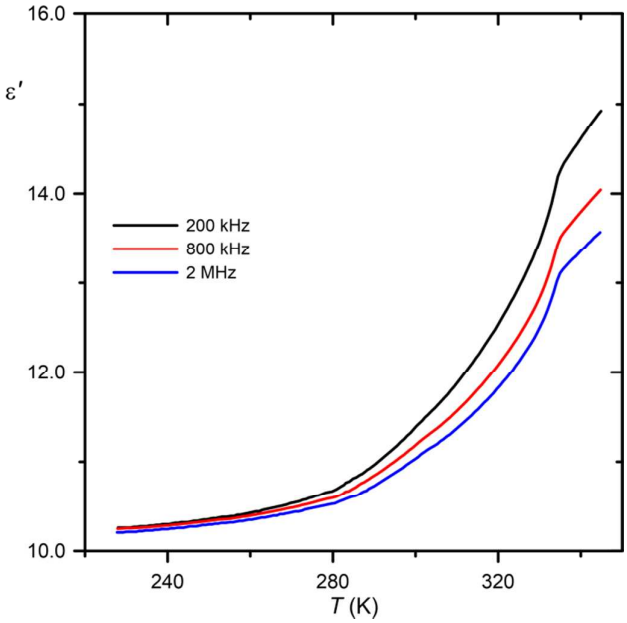

Figure 10. Temperature dependence of the real part of electric permittivity measured on the single-crystal sample of $(dabcoH_2)H_3O(BF_4)_3$ along its [z] axis, for different frequencies of electric field.

disorder contributions. However, the difference in the dielectric responses strongly suggests that in the low-temperature phase II of $(dabcoH_2)H_3O(BF_4)_3$ the oxonium cations remain disordered. The high value of ε' in this phase, below the room temperature, can originate from the dipolar fluctuations associated with the jumps of the oxonium cations between the equivalent sites in the crystal lattice. In this respect the dielectric results are consistent with the structural model of phase II, compising disordered H_3O^+ cations. This is in contrast to $(dabcoH_2)H_3O(ClO_4)_3$, where below the room temperature in phase III, the oxonium cations are ordered.

CONCLUSIONS

This study shows that dabco can form monohydrated complexes with the tetrafluoroboric and perchloric acids of the stoichiometry 1:3. In the synthesized crystals of $(dabcoH_2)H_3O(ClO_4)_3$ and $(dabcoH_2)H_3O(BF_4)_3$ the protonated water molecules are present as the oxonium cations. The ionic form of water makes these structures much more stable when compared to the similar 1:2 monohydrated complexes, where water is involved as a neutral molecule, and

which decompose around the room temperature.[16,22] Although the newly obtained crystals differ chemically only with respect to the tetrahedral ClO_4^-/BF_4^- anions, they form completely different structures. As a consequence, the phase relations and properties of these materials are also substantially different. The origin of these differences can be ascribed to the different size, mass, and moment of inertia of the ClO_4^- and BF_4^- anions, as well as to the different strength of the O–H···O and O–H···F hydrogen bonds. But the most important is the difference in the crystals packing. In particilar, in $(dabcoH_2)H_3O(BF_4)_3$ the tetrahedral anions form channels along [z] and the oxonium cations are arranged into stacks within these channels, whereas in the structure of $(dabcoH_2)H_3O(ClO_4)_3$ the arrangement of the ions is completely different. A common feature of both crystals is their high degree of disorder at elevated temperatures and the order-disorder mechanism of phase transitions. The thermodynamic parameters of the first-order phase transition between phases II and I in dabco oxonium triperchlorate, and of the second-order transition in dabco oxonium tritetrafluoroborate, make these materials interesting for practical applications in the area of energy starage and solid-state cooling.

ASSOCIATED CONTENT

Supporting Information

The Supporting Information is available free of charge on the ACS Publications website at DOI:

Thermogravimetric analysis, specific heat, structural drawing, lattice parameter as a function temperature, dielectric losses, volume thermal expansion coefficient.

Accession Codes

CCDC 1862850–1862854 contain the supplementary crystallographic data for this paper. These data can be obtained free of charge via www.ccdc.cam.ac.uk/data_request/cif, or by emailing data_request@ccdc.cam.ac.uk, or by contacting The Cambridge Crystallographic Data Centre, 12, Union Road, Cambridge CB2 1EZ, UK; fax: +44 1223 336033.

AUTHOR INFORMATION

Corresponding Author

*E-mail: masza@amu.edu.pl.

REFERENCES

(1) Żogał, O. J., Galewski, Z., Grech, E., Malarski, Z. *Mol. Phys.* **1985**, *56*, 673–681.

(2) Głowiak, T.; Sobczyk, L.; Grech, E. *Chem. Phys. Lett.* **1975**, *36*, 106–107.

(3) Katrusiak, A.; Ratajczak-Sitarz, M.; Grech, E. *J. Mol. Struct.* **1999**, *474*, 135–141.

(4) Katrusiak A.; Szafrański M. *Phys. Rev. Lett.***1999**, *82*, 576–579.

(5) Szafrański, M.; Katrusiak, A.; McIntyre, G. *Phys. Rev. Lett.* **2002**, *89*, 2155021–2155074.

(6) Szafrański, M. Bias-Field and Pressure Effects on the One-Dimensional Dielectric Response in N−H+···N Hydrogen-Bonded 1,4-Diazabicyclo[2.2.2]octane Hydrobromide Crystal, *J. Phys. Chem. B* **113**, 9479-9488 (2009).

(7) Braga, D.; Rubini, K.; Maini, L. *CrystEngComm* **2004**, *6*, 236–238.

(8) Szafrański, M.; Katrusiak, A.; Giant Dielectric Anisotropy and Relaxor Ferroelectricity Induced by Proton Transfers in $NH^{+}\cdots$N-Bonded Supramolecular Aggregates, *J. Phys. Chem. B* **2008**, *112*, 6779-6785.

(9) Szafrański, M.; Strong Negative Thermal Expansion and Relaxor Ferroelectricity Driven by Supramolecular Patterns, *J. Mat. Chem. C* **2013**, *1,* 7904-7913.

(10) Szafrański, M.; Katrusiak, A.; McIntyre, G. J.; Proton Disorder in NH···N Bonded $[dabcoH]^{+}I^{-}$ Relaxor: New Insights into H-Disordering in a One Dimensional H_2O Ice Analogue, *Cryst. Growth Des.* **2010**, *10*, 4334-4338.

(11) T. Akutagawa, S. Takeda, T. Hasegawa, T. Nakamura, Proton Transfer and a Dielectric Phase Transition in the Molecular Conductor $(HDABCO^{+})_2(TCNQ)_3$. J. Am. Chem. Soc. **126**, 291-294 (2004).

(12) Kim, Y.; Verkade, J. G. Organic-Organometallic Crystal Engineering: Novel Formation of a Honeycomb Supramolecular Architecture of $[Re_2(\mu\text{-}OMe)_3(CO)_6]^{-}$ Anions Encapsulating a Linear H-Bonded Chain of $[DABCO\text{-}H]^{+}$ Cations. *Inorg. Chem.* **2003**, *42*, 4262-4264.

(13) Wei, M.; Willett, R. D. Synthesis Crystal Structure, and EPR Studies of the Five-Coordinated $[CuCl_3(H_2O)_2]^{-}$ Complex in $(dabcoH_2)_2Cl_3[CuCl_3(H_2O)_2]\cdot H_2O$. *Inorg. Chem.* **1996**, *35*, 6381-6385.

(14) Wei, M.; Willett, R. D. A comparison of the crystal structures of $(dabcoH_2)CuCl_4$ and $(dabcoH_2)CuCl_4\cdot H_2O$. *J. Chem. Crystallogr.* **2002**, *32*, 439-445.

(15) Zhang, W.; Chen, L.-Z.; Xiong, R.-G.; Nakamura, T.; Huang, S. D. New Ferroelectrics Based on Divalent Metal Ion Alum. *J. Am. Chem. Soc.* **2009**, *131*, 12544-12545.

(15) Zhang, W.; Ye, H.-Y; Cai, H.-L.; Ge, J.-Z.; Xiong, R.-G.; Huang, S. D. Discovery of New Ferroelectrics: $[H_2dabco]_2[Cl_3]\cdot[CuCl_3(H_2O)_2]\cdot H_2O$ (dabco=1,4-Diaza-bicyclo[2.2.2]octane). *J. Am. Chem. Soc.* **2010**, *132*, 7300-7302.

(16) Szafrański, M. Comment on „1,4-Diazabicyclo[2.2.2]octane-based disalts showing non-centrosymmetric structures and phase transition behaviors" by X.-B. Han, P. Hu, C. Shi and W. Zhang, CrystEngComm, 2016, 18, 1563. *CrystEngComm* **2017**, *19*, 179-182.

(17) *Oxford Diffraction CrysAlisPro: Data Collection and Processing Software for X-Ray Diffractometers GUI, Version 4; Agilent Technologies: Santa Clara, CA,* 2010.

(18) Sheldrick, G. M. *Acta Cryst.* **2008,** *A64*, 112-122.

(19) Jona, F.; Shirane, G. *Ferroelectric Crystals*; Dover Publications Inc.: New York, 1993.

(20) Sharma, A.; Tyagi, V. V.; Chen, C.R.; Buddhi, D. Review on thermal energy storage with phase change materials and applications. *Renev. Sustain. Energy Rev.* **2009**, *13*, 318-345.

(21) Kitanovski, A.; Plaznik, U.; Tomc, U. Poredoš, A. Present and future caloric refrigeration and heat-pump technologies. *Int. J. Refrigeration* **2015**, *57*, 288-298.

(22) Han, X.-B.; Hu, P.; Shi, C.; Zhang, W. 1,4-Diazabicyclo[2.2.2]octane-Based Disalts Showing Non-Centrosymmetric Structures and Phase Transition Behaviors. *CrystEngComm* **2016**, *18*, 1563-1569.

For Table of Contents Use Only

Synthesis, Crystal Structures and Phase Transitions of Dabco Oxonium Triperchlorate and Tritetrafluoroborate

Marek Szafrański

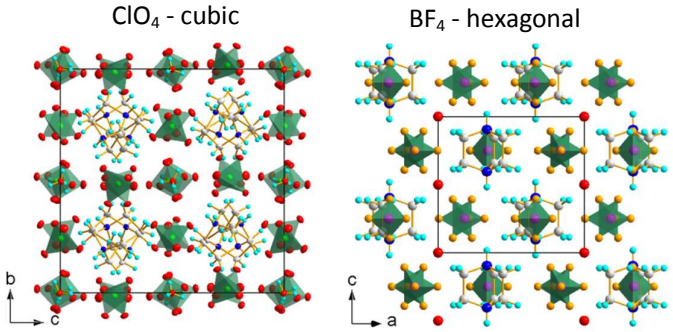

Two complexes of diprotonated 1,4-diazacyclo[2.2.2]octane and oxonium ion with perchloric and tetrafluoroboric acids have been synthesized. Their crystal structures, phase transitions, as well as dielectric and thermal properties have been characterized.